MODEL PREDICTIVE CONTROL OF A HYBRID HEAT PUMP SYSTEM AND IMPACT OF THE PREDICTION HORIZON ON COST-SAVING POTENTIAL AND OPTIMAL STORAGE CAPACITY

Francesco D'Ettorre[1] *, Paolo Conti[1], Eva Schito[1], Daniele Testi[1]

[1]**BETTER (Building Energy Technique and Technology Research Group), Department of Energy, Systems, Territory and Constructions Engineering (DESTEC), University of Pisa**

***corresponding author: francesco.dettorre@ing.unipi.it**

Abstract

The present paper analyses the cost-optimal sizing and hourly control strategy of a hybrid heat pump system for heating application, composed by an electrically-driven air source heat pump and a gas boiler. These hybrid systems represent a promising solution for the energy retrofit of existing buildings and new installations, being able to increase the efficiency of monovalent systems, especially at low external temperatures. The use of thermal storage can furtherly minimize both the operating cost and the primary energy consumption, shifting the operation of the heat pump to the most profitable periods. In this work, the optimal control problem has been investigated by means of mixed-integer linear programming, considering an ideal forecast of external temperature and thermal load on given horizon periods (i.e. model predictive control). Achievable cost savings with respect to a traditional rule-based control strategy with no storage are presented as a function of both prediction horizon and storage capacity in a dimensionless form. A relation between prediction horizon length and optimal storage capacity is shown. An example of application of the method is illustrated, showing cost savings up to 8%. A sensitivity analysis on the storage tank losses, climatic conditions, generators efficiency, and energy prices is also presented, showing the cost saving potential in all these different conditions.

Keywords: hybrid heat pump; model predictive control; MILP; thermal energy storage, forecasting horizon; optimal operation.

1 Introduction

It is well known that the building sector is one of the main energy user in the European Union, being responsible for 25.4% of the final energy consumption [1], most of which is consumed for space heating purposes in residential buildings. The latter constitute the 75% of the EU's building stock and nearly half of it has been built before the 1960s, without particular consideration of building envelopes and energy systems performance levels, thus it contributes to the higher energy consumption of the sector. In this context, hybrid systems can be considered an attractive solution to fulfil the EU Directive 2010/31/EU on energy performance of buildings, which states that all new buildings have to be nearly Zero Energy Buildings from 2018/2020 [2], as well as the EU Directive 2012/27/EU on energy efficiency, being the heat source used by the heat pump considered as renewable [3]. These hybrid systems are composed by an electrically-driven heat pump coupled with a secondary heat generator, which can be either a gas boiler or an electrical heater. The generators can be operated, according to the chosen control strategy and system configuration, either simultaneously or alternatively [4]. This means that differently from monovalent heat pump systems, in hybrid systems the heat pump can be sized to cover a fraction of the maximum thermal load. In this way, the heat pump can be operated during the heating season with higher load factors, reducing the annual cycling losses [7] and increasing the seasonal performance factor (SCOP). Furthermore, thanks to the second generator, all the worst heat pump working conditions during the year (e.g., when the external temperatures get their lower values) can be avoided, increasing the overall system performances. This explains the research efforts conducted over the last few decades on this kind of systems. Bagarella et al. studied the effects of both the cut-off temperature and the heat pump size on the annual energy performance of a hybrid heating systems for residential buildings [6,7]. They also compared two different system configurations (bivalent parallel plant vs. alternative parallel plant), in order to determine which one leads to the higher energy saving. Di Perna et al. studied experimentally the performances of a hybrid heat pump-gas boiler generator for heating purposes [8]. Li et al. analysed the effects of the operational strategy of a multiple sewage-source heat pump and gas boilers on the annual energy consumption and cost [9]. Scarpa et al. simulated the performances of a hybrid system for hot water generation, composed by a solar-assisted heat pump coupled with a gas burner [10]. Qi et al. provided an overview on the status and developments of hybrid energy systems [11].

Furthermore, several studies have also been conducted on hybrid heat pump systems coupled with both active and passive thermal storage devices, since it has been proven that the latter can increase the system performances, especially when coupled with advanced optimization-based control strategies as model predictive control (MPC). Renaldi et al. presented the design and operational optimization of a residential heating system, composed by a heat pump coupled with a water thermal storage, by means of mixed-integer linear programming (MILP). They also compared the total cost of the heat pump system with that of a traditional gas boiler, showing a cost saving going from 5% up to 37%, according to the adopted emission system (radiator or floor heating system) [12]. Pardo et al. studied the optimal configuration of a hybrid cooling system composed by a ground source heat pump, an air source heat pump, and a storage device, showing that the electricity consumption of the hybrid system achieves 60% and 82% when compared with a system with only the air-source heat pump or the ground-source heat pump, respectively [13]. Yu et al. presented a review of the control strategy using thermal energy storage (TES) into different building systems [14].

Research on MPC has focuses on different aspects. Several studies have been conducted on the optimal control of passive storage devices, as building thermal mass or floor heating system [15-17], whose high inertia makes the adoption of MPC particularly appropriate. Other studies have focused on the demand-side potential, being the thermal storage device able to shift the heat pump operation towards times with low rate electricity prices [18-20]. Another important aspect is the optimal control problem formulation, since it is one of the most critical point in the design and practical implementation of the controller. Verhelst et al. studied the effects of different cost-function formulations on the optimal control of an air-water heat pump connected with a residential floor heating system, showing that the operating costs are strongly affected by problem formulation [21-22]. Schütz et al. presented a comparison between different storage models adopted with mixed-integer linear programming in order to define the cost-optimal control strategy of a monovalent heating system coupled with a TES [23]. Cole et al. studied the effect of the width of the control horizon on the performance of a MPC implemented in a building with passive thermal storage [24]. Oldewurtel et al. and Sturzenegger et al. showed a correlation between the prediction horizon and the building thermal mass, suggesting that the former should be chosen on the basis of the time constant of the building [25-26]. Halvagaard et al. showed the effect of the prediction horizon length on the performance of a water storage tank coupled with a solar panel for heating application, concluding that the controller performances are influenced by the prediction horizon until the system constraints (storage capacity, maximum solar panel power) become dominant, limiting the achievable cost-saving [27]. In this context, the present study focuses on the optimal control of a hybrid heating system, composed by an air-to-water heat pump, coupled with a gas boiler and a sensible water-storage tank for space heating application. The objective of the work is the application of the MPC on this typology of system and the evaluation of possible correlation between the predicted horizon and the optimal storage capacity. To the authors' best knowledge, this topic has never been addressed in literature and can provide useful information for the design of such systems, in order to avoid an uneconomically oversized storage volume and to implement a more efficient predictive controller. In order to address the main issues concerning the present work, the following steps are considered.

First, the hybrid generator model is presented. Heat pump performances, which is generally a critical issue, being strongly influenced by external temperature and load factor, are evaluated by means of an experimentally-validated expression. Then, in order to define the optimal system operation, a MPC approach using mixed-integer linear programming (MILP) is presented. To fully investigate the potential of the MPC applied to the system under investigation, underling the effects of both the storage capacity and the prediction horizon, an ideal reference case, in which the storage device is considered perfectly insulated is firstly analysed. Several simulation runs have then been performed, varying both the storage capacity and the forecast window over which the control strategy is optimized. Results are compared, in a dimensionless form, to those of a baseline case without thermal storage. Afterwards, starting from the optimal solution of the ideal case, the effects of both the storage losses and the external temperature profile have been taken into account and a reference trade-off solution for the storage capacity with heat losses has been identified. Finally, starting from this latter case, a sensitivity analysis to energy prices and efficiencies of the generators has also been conducted.

2 Methodology

2.1 Systems overview and modelling

A schematic diagram of the system is reported in Fig.1. A hybrid generator composed by an air-to-water electrically-driven heat pump with variable capacity control units coupled with a gas boiler was considered. The two generators are operated in parallel mode, being this one the most widespread solution in existing applications [5]. In the baseline case (Fig.1 in black), without thermal energy storage, a control unit establishes which generator should be activated to meet the load, on the basis of minimum-cost criteria and the operating ranges of the generators. A thermal storage tank is then considered connected in parallel to the hybrid generator (Fig.1 in red), with the purpose of decoupling energy generation from energy distribution, taking advantages of the best possible working conditions for the heat pump. For this purpose, a predictive controller is implemented to define the cost-optimal control strategy of both generators and the storage tank. The typical time-step adopted both for modelling the system components and implementing the control actions is an hour.

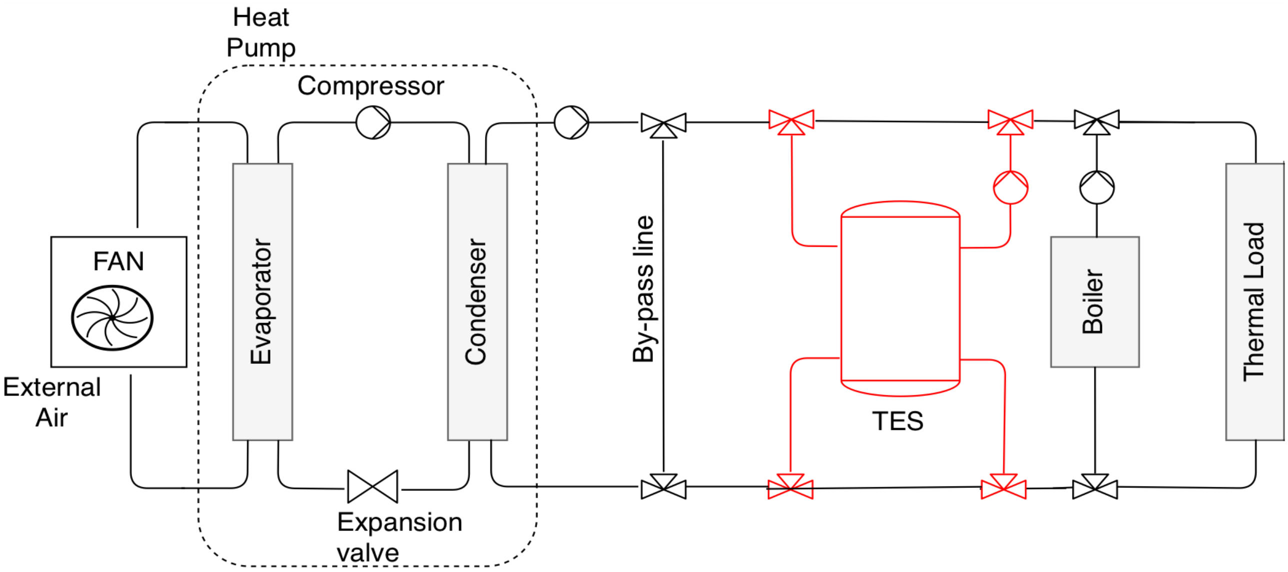

Figure 1: System layout.

2.1.1 Heat pump model

As suggested by several technical standards (see, for instance, EN 15316-4-2) the so-called second-law efficiency (η^{II}) is used to evaluate the heat pump performance. The latter reads:

$$COP = \eta^{II} COP_{id} \tag{1}$$

where COP_{id} is the coefficient of performance of a reversed Carnot cycle, calculated by means of the source and sink temperatures as:

$$COP_{id} = \frac{T_{sink}+273.15}{T_{sink}-T_{source}} \tag{2}$$

The evaporation temperature (T_{source}) is considered equal to the external air temperature (T_{ext}), while the condensation temperature depends on the service provided. If the heat pump is operated to charge the storage, the condensation temperature (T_{sink}) is considered equal to the maximum storage temperature (T_s^{max}), otherwise, when the heat pump directly serves the load, it is considered equal to the distribution supply temperature (T_{supp}^L). To evaluate the second low efficiency η^{II}, the effects of both the lift between the source and sink temperatures and the part load conditions must be taken into account. The latter, by means of its load factor LF_{HP}, is considered equal to the ratio between the thermal power delivered by the heat pump $\dot{Q}_{HP}$ and its maximum power $\dot{Q}_{HP}^{max}$. To this end, the following dimensionless parameters are introduced:

$$\beta = \frac{T_{sink}+273.15}{T_{source}+273.15} \tag{3}$$

$$LF_{HP} = \frac{\dot{Q}_{HP}}{\dot{Q}_{HP}^{max}} \tag{4}$$

The second low efficiency is represented by means of a polynomial, based on a fit of experimental data (details on the experimental characterization of the heat pump performances are reported in Appendix A):

$$\eta^{II} = c_0 + c_1\beta + c_2 LF_{HP} + c_3\beta^2 + c_4\beta \cdot LF_{HP} \tag{5}$$

In this way, the heat pump performances can be finally evaluated throughout the operative range and for each value of the source and sink temperatures, combining Eq. (2) and Eq. (5) as:

$$COP = (c_0 + c_1\beta + c_2 LF_{HP} + c_3\beta^2 + c_4\beta \cdot LF_{HP}) \cdot \frac{T_{sink}}{T_{sink}-T_{source}} \tag{6}$$

2.1.2 Gas boiler model

In the present work, the boiler performance is modelled by means of a constant efficiency (η_{boil}) over the whole operative range.

2.1.3 Thermal storage tank model

The water storage is modelled as a perfectly-mixed storage tank located outside of the heated volume of the building. Under these assumptions, the evolution of the state of charge of the storage tank can be calculated from the following energy balance:

$$\rho V c \frac{dT_s}{dt} = \dot{Q}_{HP,S} - \dot{Q}_{S,L} - \dot{Q}_{loss} \tag{7}$$

where ρ is the water density, V the storage volume, c the specific heat of water, $\dot{Q}_{HP,S}$ is the heat delivered by the heat pump to the storage, $\dot{Q}_{S,L}$ is the energy delivered per unit time by the storage to the load, and $\dot{Q}_{loss}$ are the heat losses to the surrounding ambient. The latter are calculated as:

$$\dot{Q}_{loss} = UA(T_s - T_{ext}) \tag{8}$$

where (UA) is the overall heat transfer coefficient of the storage, which is considered proportional to the size of the tank when different storage capacities are taken into account. Moreover, the assumption of direct inflow within the storage tank has been made. During the charging process, the water within the storage is heated by the mixing process with the hot water coming at constant temperature (equal to the maximum storage temperature) from the condenser of the heat pump.

2.1.4 Thermal load

Being the present work focused on the control strategy of the hybrid generator, we consider the thermal load ($\dot{Q}_{load}$) only as a boundary condition of our problem, which we assume to be known in advance on a given horizon. This means that the storage tank capacity comes down to be the only source of flexibility of the system. To this end, the thermal energy required by a single dwelling on a typical winter day is considered. The thermal load is evaluated as a function of the external temperature (T_{ext}) by means of the energy signature method (see annex B of standard EN 15603:2008 [28]), whose parameters have been chosen in such a way that the thermal load reaches the design value ($\dot{Q}_{load}^{des}$) when the external temperature gets to the design outdoor temperature (T_{des}) and becomes zero at the switch-off temperature (T_{off}), at which building gains and losses are balanced and the heating system is turned off.

$$\dot{Q}_{load}(t) = \dot{Q}_{load}^{des}\left(1 - \frac{T_{ext}(t-\phi) - T_{des}}{T_{off} - T_{des}}\right) \tag{9}$$

Moreover, to take into account the time delay between the heat demand and the evolution of the outdoor temperature, a characteristic time shift (ϕ) of the building has been introduced, according to [29,30].

2.1.5 Climatic data

To evaluate the thermal load and implement the predictive control strategy, a forecast model of the external temperature needs to be used. The latter can be assumed with a sinusoidal profile, which can be conveniently extended to match any temperature evolution by the Fourier series method:

$$T_{ext}(t) = \tilde{T}_{ext} + \Delta T \sin\left(\frac{2\pi}{24}t + \phi\right) \tag{10}$$

where t is the hour of the day and $\tilde{T}_{ext}$, ΔT and ϕ are respectively the mean value, the amplitude and the phase shift of the daily outdoor temperature profile.

2.2 Control strategy

2.2.1 System without TES (baseline case)

In the baseline case, a rule-based control (RBC) strategy applies: the cost-optimal control strategy is obtained by operating at any time the more cost-effective generator. To this end, a control unit compares the COP of the heat pump with a COP of economic equivalence (COP_{eq}), calculated on the basis of the cost of energy and the efficiency of the gas boiler. Defined p_e [€/kWh] and p_{gas} [€/kWh], respectively, as the prices of electricity and natural gas, the COP_{eq} is defined as:

$$COP_{eq} = \frac{p_e}{p_{gas}}\eta_{boil} \tag{11}$$

If the heat pump economic performance is higher than that of the condensing boiler ($COP > COP_{eq}$) and it has enough capacity to supply the required thermal load, the heat pump is operated and the boiler is switched off, otherwise, the heat pump is turned off and all the energy is supplied by the boiler.

2.2.2 System with TES

When the storage tank is considered, differently from the rule-based control (RBC) strategy of the baseline case, the target of the control action is to find at each time step how to operate the two generators in order to minimize the operating cost of the system from the present to the end of the available prediction horizon, hence considering not only the required thermal load at a given time, but also the information about the future. To this end, a model predictive control (MPC) is implemented and an optimization problem is formulated and solved within a finite optimization window at each control time step. Details on the optimal control problem (OCP) formulation are reported in section 3.

2.3 Simulation

To fully explore the potential of the system and underline the relation between the predictive control strategy and the storage capacity, several simulation runs have been performed and compared, varying both these parameters. A periodic daily thermal load has been imposed, also assuring the equivalence between initial and final state of the storage tank. This has been done with the two-fold aim of avoiding results affected by transient conditions and to underline how the chosen prediction horizon affects the control strategy and consequently the achievable cost-saving.

3 Optimal control problem formulation

Model predictive control is a method of control, which, compared to traditional controllers (see for instance PID controller), is able to evaluate the control action taking into account not only the state of the system at the considered control time-step, but also information about future events that can affect the system behaviour. In the present work, perfect forecasts of the external temperature have been considered. At each time-step (in our case, one hour long), the control action is evaluated solving an open loop optimal control problem, in which an objective function is minimized over a finite control horizon of N hours. Once the OCP is solved, only the first element of the control trajectory is implemented by the controller and the state of the system is evaluated according to the implemented control action, then moving the system to the next control time-step during which the same process is repeated.

In the present paper, the cost of the energy produced by the two generators to meet the building thermal demand over the control horizon N is adopted as the objective function. The control variables are the hourly j-th values of the load factors of both the heat pump ($LF_{HP,j}$) and the gas boiler ($LF_{B,j}$, defined as the ratio between the thermal power delivered by the boiler and its maximum thermal power $\dot{Q}_B^{max}$), over the considered horizon, the thermal power delivered by the storage tank ($\dot{Q}_{S,L,j}$), and the two binary variables δ_L and δ_S, describing the working state of the heat pump. If the heat pump is charging the storage tank, then $\delta_S = 1$ and $\delta_L = 0$, and vice-versa otherwise.

$$min J = \sum_{j=1}^{N} \left(\frac{p_{el}\dot{Q}_{HP}^{max}}{COP_{L,j}} LF_{HP,L,j}\delta_{L,j} + \frac{p_{el}\dot{Q}_{HP}^{max}}{COP_{S,j}} LF_{HP,Sj}\delta_{S,j} + \frac{p_{gas}\dot{Q}_{B}^{max}}{\eta_{boil}} LF_{B,j} \right) \Delta t \qquad (12)$$

with $COP_{L,j}$ and $COP_{S,j}$ the heat pump coefficients of performance related to the two different operating conditions.

In this way, two mutually exclusive operating conditions can be taken into account, introducing the following constraint on those binary variables:

$$\delta_{L,j} + \delta_{S,j} = 1 \;\forall\, j \in [1, N] \tag{13}$$

It should be noticed that, due to the product between the control variables (the binary variables and heat pump load factors), the problem formulation is not linear. Notwithstanding this, using classical linearization techniques, the problem can still be formulated as a mixed-integer linear programming problem.

To take into account the operative range of both generators, the following constraints are imposed. The heat pump is considered able of modulating its capacity down to a given fraction of its maximum value (LH_{HP}^{min}). Furthermore, we also consider that the heat pump cannot be operated if the external temperature is below a chosen threshold value (T_{cutoff}). On the other hand, the gas boiler is considered capable of modulating its capacity with a constant efficiency at whatever load factor from 0 to 1.

$$LH_{HP}^{min} \le LF_{HP,j} \le 1 \qquad if\ T_{ext,k} \ge T_{cutoff} \tag{14}$$
$$LF_{HP,j} = 0 \qquad if\ T_{ext,k} < T_{cutoff} \tag{15}$$
$$0 \le LF_{B,j} \le 1 \qquad \forall\, j \tag{16}$$

Furthermore, we consider that the thermal energy required by the load must always be supplied, leading to:

$$\dot{Q}_{HP}^{max} LF_{HP,j} + \dot{Q}_{B}^{max} LF_{B,j} + \dot{Q}_{S,L,j} = \dot{Q}_{load,j} \qquad \forall\, j \tag{17}$$

As usual in optimization contexts, the differential equation (6) describing the evolution of the storage temperature is implemented as a state constraint. This is done to take into account boundary conditions on the storage temperature and to avoid withdraws from the storage when its temperature is below the supply water temperature required by the emission system (T_{em}). A condition is introduced to ensure that the thermal energy delivered by the storage during the whole time-step (Δt) does not exceed the useful energy stored. The upper and lower bounds (T_s^{max}, T_s^{min}) of the storage temperature are set respectively equal to the maximum supply temperature that the heat pump can provide and the value of the outdoor temperature.

$$T_{s,j}^{min} \le T_{s,j} \le T_{s,j}^{max} \quad \forall\, j \tag{18}$$
$$\dot{Q}_{S,L,j}\Delta t \le \rho V c \left(T_{s,j} - T_{em}\right) \quad \forall\, j \tag{19}$$
$$\dot{Q}_{S,L,j} = 0 \quad if\ T_{s,j} < T_{em} \quad \forall\, j \tag{20}$$

4 Performance indexes

To enforce the model applicability, results are presented in dimensionless form by means of the following performance indexes. The dimensionless storage capacity (SC) is considered as the ratio between the maximum useful energy that can be stored (E_{useful}^{max}) and the daily energy required by the load $\left(E_{load}^{daily}\right)$:

$$E_{useful}^{max} = \rho V c (T_s^{max} - T_{em}) \tag{21}$$
$$E_{load}^{daily} = \sum_{j=1}^{24} \dot{Q}_{load,j}\, \Delta t \tag{22}$$
$$SC = \frac{E_{useful}^{max}}{E_{load}^{daily}} \tag{23}$$

A parameter which identifies the storage state of charge (SoC) is defined as:

$$SoC(t) = \frac{E_{useful}(t)}{E_{useful}^{max}} \tag{24}$$

with $E_{useful}(t)$ the storage energy content at time t, evaluated by using $T_s(t)$ instead of T_s^{max} in Eq. (21).
The prediction horizon N is normalized taking one day as the reference scale for time ($\tau_o = 24h$):

$$\tau = \frac{N}{\tau_o} \tag{25}$$

Finally, the global cost saving (CS) is evaluated for each case as the relative difference between the cost of heating in the considered case and the cost of heating in the baseline case without the thermal storage device:

$$CS = 1 - \frac{cost\ of\ heating}{(cost\ of\ heating)_{baseline}} \tag{26}$$

5 Application of the method

A hybrid heat pump-boiler generator coupled with a sensible TES to be installed in a dwelling with an underfloor heating system is modelled in accordance with the method described in the previous paragraphs. The heating load of the building is 6 kW at the design external temperature $T_{des} = -5\ °C$ and a room temperature of 20 °C, while it becomes zero at the switch-off temperature $T_{off} = 18\ °C$. The mean external temperature is 8.5 °C and the amplitude of its sinusoidal profile is 6.5 °C. The daily thermal energy need is 91 kWh, evaluated on the basis of the load profile resulting from Eq. (9). The emission system is considered as flow controlled; this means that the heat flow is supposed to be controlled varying the flow rate, while the supply temperature from the hybrid generator or from the storage tank is kept constant. To this end, the emission supply water temperature is considered constant and equal to 35 °C. The generation supply temperature is considered equal to the maximum storage temperature when it is supplied by the heat pump to the storage tank and equal to the emission supply temperature when it is supplied either by the heat pump or by the gas boiler directly to the thermal load. Moreover, the heat pump (nominal power: 8 kW) is considered able to modulate its load factor down to 0.2, while the threshold value below which the heat pump is turned off is chosen equal to 5 °C. The maximum storage temperature is considered equal to 45 °C. The boiler is sized to meet the load demand at any time (peak power: 6 kW) and it is able to modulate its power output at a constant efficiency, set equal to 0.96. Simulations were run over a period of a week with a time resolution of 1 hour and a prediction horizon N equal to the control horizon. The employed values of N are 1, 3, 6, 9, 12, and 24 hours. All the simulations have been carried out firstly in an ideal reference scenario, in which the storage tank is considered as perfectly insulated. The electricity price is considered equal to 0.20 €/kWh and the one of natural gas equal to 0.08 €/kWh. Afterwards, a sensitivity analysis on both the level of insulation of the storage tank, the profile of the outdoor temperature, and the electricity price have been conducted.
In the present section, results are presented in the following way. Firstly, referring to the ideal reference case, the effects of the storage capacity and width of forecast window are analysed, highlighting how they affect both the achievable cost saving and the system performances. Afterwards, a sensitivity analysis is performed on the values of thermal losses, external temperature

profile, and energy prices. Table 1 summarise the characteristics of the building load demand and of the generators.

Parameters	Value
Peak load demand [kW]	6
Building time-shift [h]	6
Daily energy demand [kWh]	91.2
Design outdoor temperature [°C]	-5
Switch-off outdoor temperature [°C]	18
HP nominal power [kW]	8
Outdoor temperature threshold value [°C]	5
Boiler nominal power [kW]	6
Boiler efficiency	0.96

Table 1: Characteristics of the building load demand and of the generators.

5.1 Impact of storage capacity and width of the forecast window on the maximum achievable cost saving for the ideal reference case

Fig. 2 shows, for the ideal reference case ($UA = 0$), the achievable cost saving as a function of both the dimensionless storage capacity (SC) and forecast window (τ). It can be seen that, regardless of the value of τ, an increase in the storage capacity always leads to a reduction in the energy cost. Nevertheless, this positive effect rapidly tends to saturate, as soon as the storage capacity gets close to the daily energy load. It can also be observed that the predictive ability affects the cost-saving in a more substantial way compared to the storage capacity. A saturation effect on the achievable cost saving with the length of the prediction horizon is also noticed. This effect can be explained considering how the forecast capability affects the cost-effectiveness of the control strategy. Thanks to the forecast, the controller is capable to schedule the generators on the basis of the prediction of both the load and the external temperature profiles, and consequently of the heat pump efficiency. As a result, if a TES is present, the controller can operate a load-shift to exploit the most profitable working conditions of the heat pump. To this end, the heat pump is forced to work during the hours of the day with the highest outdoor temperature, to anticipate the production of a fraction or all the thermal energy required by the load at the hours of the day when the outdoor temperature gets its lower values and the heat pump is less effective than the gas boiler. Moreover, it should be noticed that an increase in the length of the forecast window increases the controller capability to detect the worst conditions of the day, which in turn affects the amount of energy that should be shifted. Consequently, an increment in the value of τ corresponds to an increment in the amount of energy that should be shifted. Notwithstanding this, the amount of energy that can be shifted is strictly connected to the capacity of the TES, and for this reason a saturation effect on the cost saving occurs as the forecast window increases, since, once the energy that should be shifted equals the TES capacity, no further load-shifting is allowed and consequently no further cost saving will occur.
Indeed, a strong correlation between the storage capacity and the predictive ability is pointed out. This means that the predictive ability should be taken into account in the choice of the storage capacity and vice-versa, in order to avoid an uneconomically oversized storage volume and, to the other hand, to implement a more efficient predictive controller.

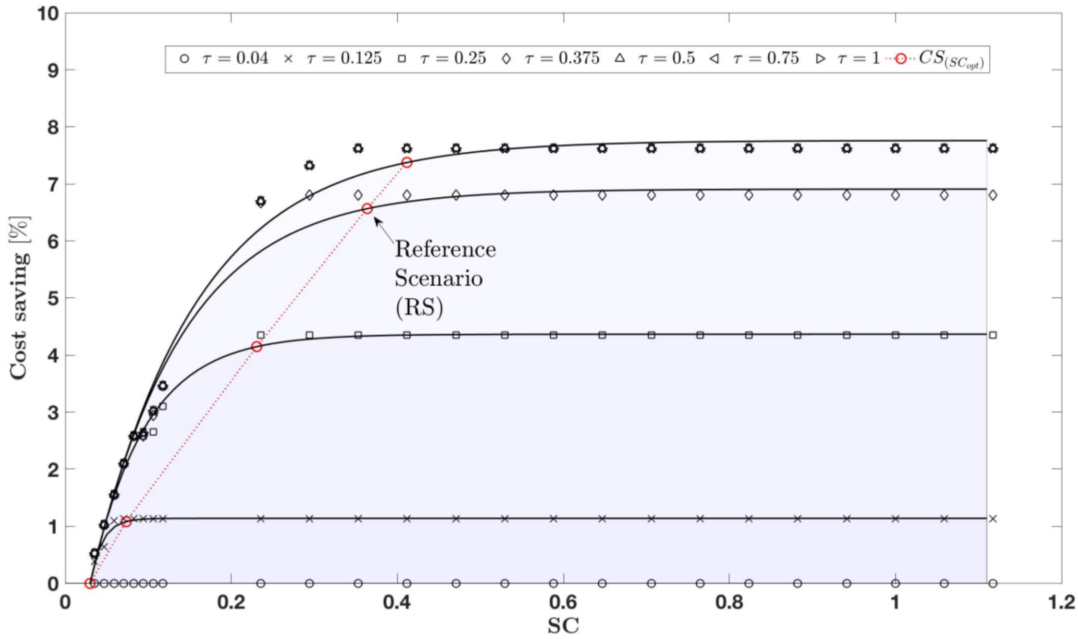

Figure 2: Cost saving (CS) as a function of the storage capacity (SC) for different predictive abilities (τ).

The above-mentioned correlation, shown in Eq. (27), has been obtained considering the optimal storage volume (SC_{opt}), as this storage capacity corresponds to a cost saving equal to 95% of its maximum value for each value of τ. In other words, storage volumes higher than SC_{opt} produce a cost-saving increment lower than 5% (red line in Fig. 2).

$$SC_{opt} = \ 0.43 \cdot \left(1 - e^{-6.25\cdot(\tau - 0.1)}\right) \tag{27}$$

Results are shown in Fig. 3, where the optimal values of the storage capacity defined above and the corresponding optimal cost savings are plotted against the width of the prediction horizon (τ). In this way, once a prediction capability has been chosen, the corresponding SC_{opt}, can be immediately assessed and, consequently, the maximum achievable cost saving, according to Eq. (28).

$$CS = \ CS_{max} \cdot [0.19 \cdot \left(1 - e^{-6.17\cdot(\tau - 0.1)}\right)] \tag{28}$$

CS_{max} is a theoretical cost saving that would be achieved if the heat pump always supplied all the load with its maximum efficiency. The latter value is considered as the COP occurring during the best hour of the day, with the highest predicted outdoor temperature and at full load conditions.

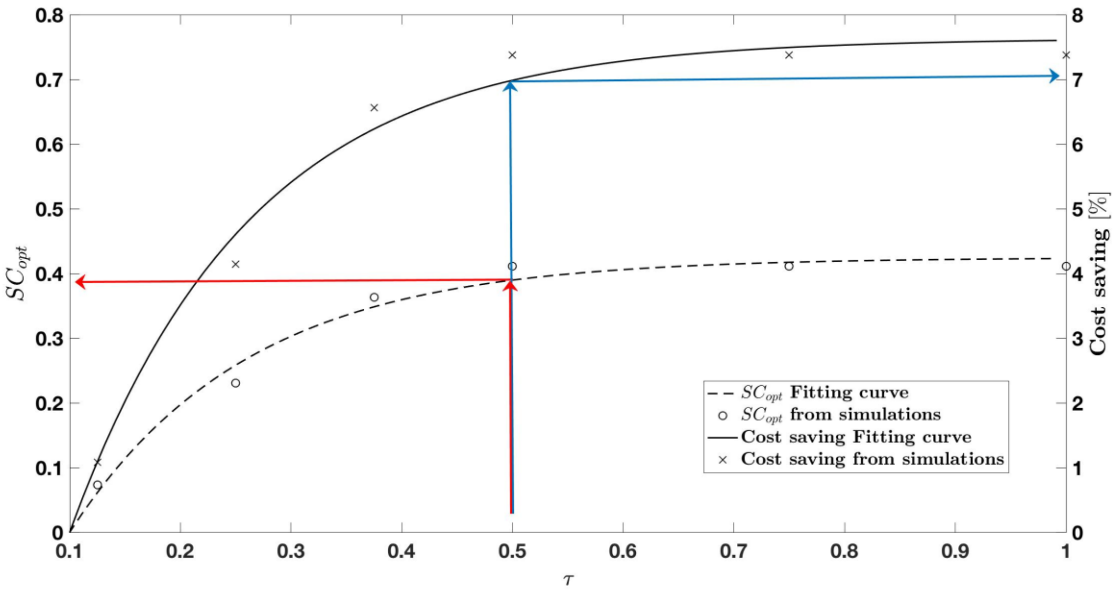

Figure 3: Achievable cost saving and SC_{opt} as a function of the predictive ability (τ).

5.2 Analysis of the optimal control strategy in a reference case

Let us now define a reference case with a given storage capacity and predictive ability, to illustrate the optimal control strategy (next, on the same case, we will perform the sensitivity analysis). As reference scenario (RS), we choose SC=0.375 and τ=0.375, being a possible trade-off between investment and achievable cost saving (see Fig. 2). Figs. 4-5 compare the control strategy of the RBC adopted in the baseline case, without storage device, with that of the MPC for the reference case. In the baseline case, the heat pump is operated most of the time, when the outdoor temperature is above the cut-off value and the COP is higher than COP_{eq}. The gas boiler is then operated to match the load during the night, when the heat pump would work in its worst operative conditions and the thermal load reaches its higher values. On the other hand, when a storage device is considered within the system and a predictive control strategy is adopted, the operations of both generators drastically change (the share of the daily thermal load covered by the boiler drops from 35.3% to 20%). In fact, almost all the thermal energy required by the load is now produced by the heat pump, using more cost-effective working conditions. The different operation of the gas boiler can also be noticed, being mainly operated to deliver energy to the building during the hours in which the heat pump charges the storage, in view of the night-time load. In fact, during the night, the gas burner is turned off and all the load is supplied by the storage tank.

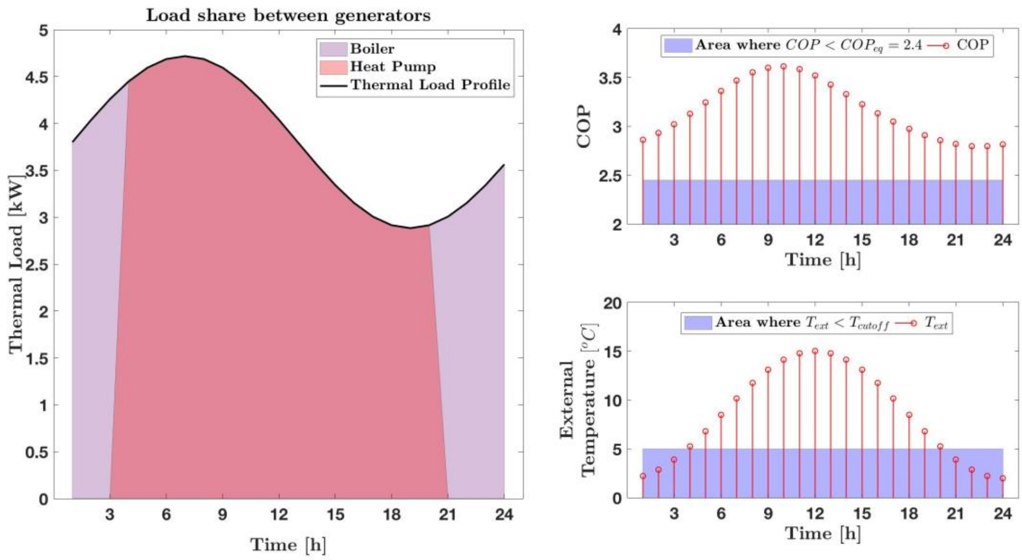

Figure 4: Optimal control of the generators of the hybrid system in the baseline scenario.

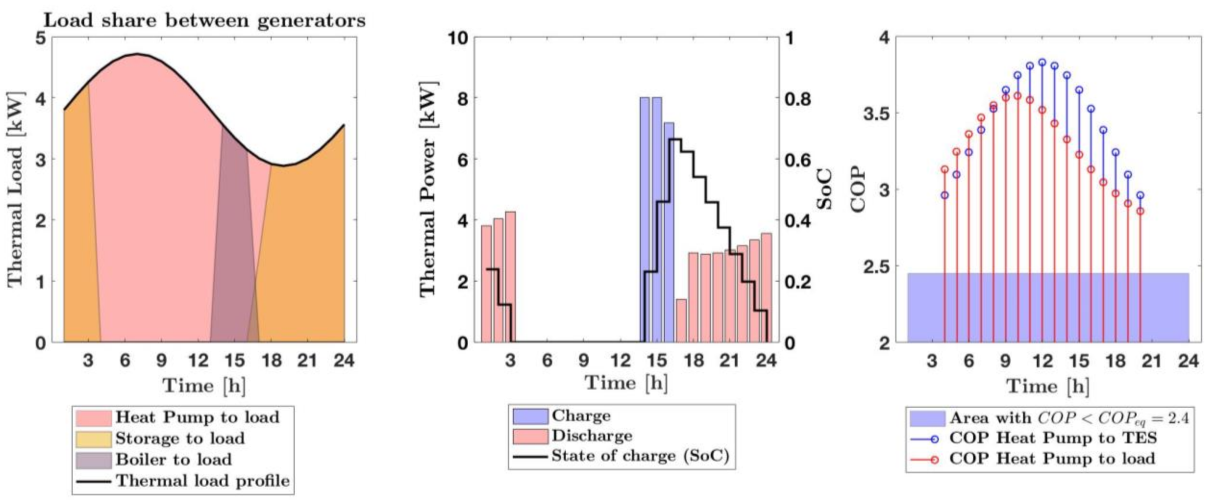

Figure 5: Optimal control of the generators of the hybrid system in the reference scenario with MPC.

5.3 Impact of the storage losses

To investigate how the level of storage insulation affects the system performances, further simulations have been conducted, considering the water-storage tank insulated in a way that the average daily heat losses are no more than 3%, 5%, 8%, and 10% of the maximum useful energy that can be stored. Results are shown in Fig. 6. Differently from the reference scenario in which the storage device is considered perfectly insulated and the achievable cost saving tends to saturate with the storage capacity, when thermal losses are considered, an optimal cost-saving point occurs, after which the cost saving decreases. This is due to the fact that the energy required by the generation system for balancing the thermal losses increases proportionally with the storage volume; also, the useful energy that can be stored increases, but it is limited by the maxim energy that the heat pump can provide, which depends on both the heat pump capacity and the period of time during which the heat pump works in profitable conditions. Consequently, while the useful energy tends to saturate, the energy required to compensate the thermal losses monotonically increases as the storage capacity increases, leading to a less cost-effective performance of the system.

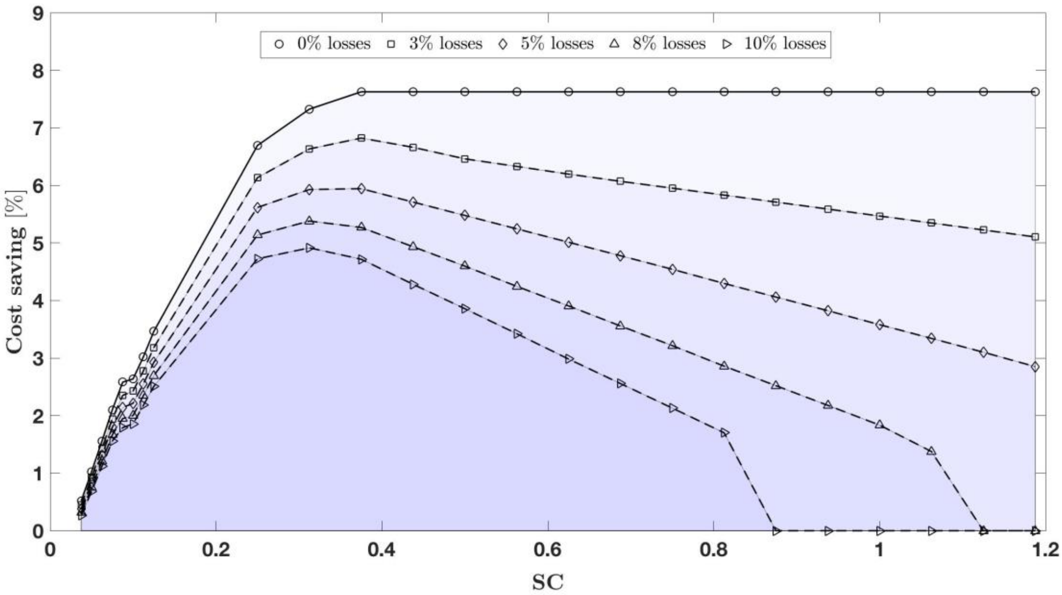

Figure 6: Cost saving as a function of the storage capacity, for different values of the average daily thermal losses.

5.4 Impact of the external temperature profile

Considering as reference case, being a good practical trade-off solution, the configuration derived in the previous analysis with 3% storage losses, storage capacity SC=0.375, and prediction horizon τ=0.5, the effects of the outdoor temperature profile have been analysed, varying both its mean value between 5.5°C and 10°C with 1.5 °C step and its amplitude between 0 °C and 7.5 °C. The daily energy demands related to the adopted values of the mean outdoor temperature are equal to 101.4 kWh, 96.3 kWh, 91.2 kWh and 86.1 kWh, respectively. The sensitivity analysis, reported in Fig. 7, shows that, for low amplitudes, the cost saving increases only at low outdoor temperature mean values. In fact, the controller uses the thermal storage only if some hours of the day have a temperature lower than 5 °C (i.e., heat pump cut-off), as the advantages arising from operating the heat pump during the hours with high outdoor temperatures are less significant compared to the COP degradation due to the higher supply temperature needed to charge the storage (T_s^{max} instead of T_{em}). At high average temperatures and low amplitudes, the outdoor temperature is always above the cut-off value and the most profitable operative strategy coincides with the no-TES configuration.

Tables 2-4 show the load-share between the two generators, which is reported for both the studied configurations and for three different values of the amplitude of the outdoor temperature (low, medium, and high). We note that the advantages of using the TES configuration is related to the lower load fraction delivered by the boiler and the higher use of the thermal storage.

Table 2 shows the minor deviation with respect to the no-TES configuration. Only in the case of $\tilde{T}_{ext} = 5.5$ °C and $\Delta T = 1$ °C we note a 50% reduction in the energy delivered by the heat pump directly to the load, while no differences are observed between the two configurations if the outdoor temperature remains above the cut-off value. In this case, the total load share covered by the heat pump globally rises, moving from 62% to 77%, the energy delivered by the heat pump directly to the load decreases from 62% to 31%, and the storage rises its contribution from 0% to 46%.

The load-shifting advantages are more relevant in the cases shown in Tables 3 and 4. In the case of $\tilde{T}_{ext} = 8.5$ °C and $\Delta T = 4$ °C, the boiler share and the energy delivered by the heat pump directly to the load are reduced of 5% and 30%, respectively. In the case of $\tilde{T}_{ext} = 10$ °C and $\Delta T = 4$ °C, the load-share directly covered by the heat pump decreases from 100% to 48%, while the heat load delivered by the thermal storage is equal to 37%. The boiler meets the 15% of the energy demand, as the heat pump cannot meet the load during the charging phases of the storage.

Finally, as shown in Table 4, when an even higher amplitude is considered ($\Delta T = 7.5$ °C), the cost saving increases as the mean outdoor temperature increases. In these cases, a high value of the mean temperature entails low values of the daily thermal loads and, consequently, low load factors and COP values, if heat is directly supplied to the building. In these conditions, the presence of a storage device allows the operation of the heat pump at the most profitable external conditions and with high load factors, thus reducing the daily operating cost of the system.

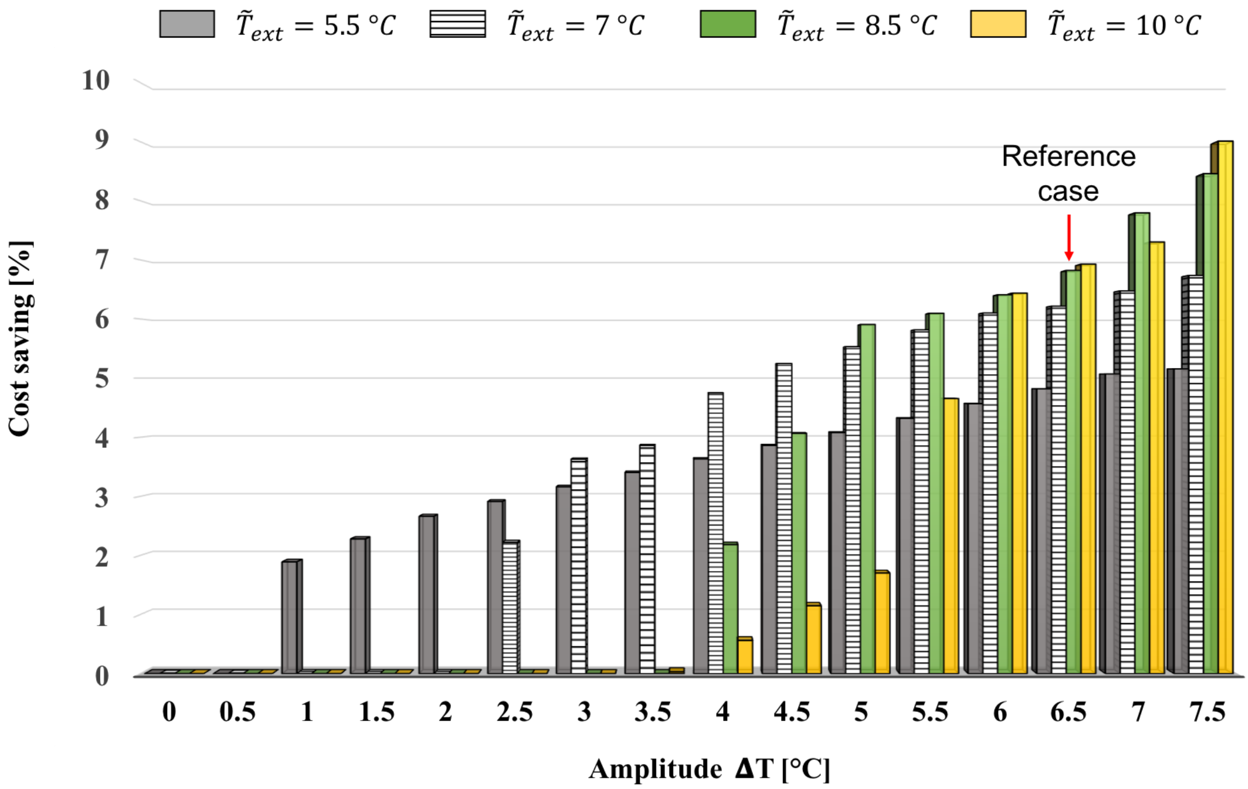

Figure 7: Impact of the external temperature profile on the achievable cost saving with respect to the NO-TES configuration.

$\tilde{T}_{ext}$ [°C]	E_{load}^{Daily} [kWh]	Load share without TES		Load share with TES		
		Heat Pump	**Boiler**	**HP to Load**	**HP to TES**	**Boiler**
5.5	101.4	62	38	31	46	23
7	96.3	100	0	100	0	0
8.5	91.2	100	0	100	0	0
10	86.1	100	0	100	0	0

Table 2: Load share between the two generators for the configuration with and without TES - Amplitude $\Delta T = 1$ °C.

$\tilde{T}_{ext}$ [°C]	E_{load}^{Daily} [kWh]	Load share without TES		Load share with TES		
		Heat Pump	**Boiler**	**HP to Load**	**HP to TES**	**Boiler**
5.5	101.4	55	45	39	31	30
7	96.3	63	37	40	40	20
8.5	91.2	80	20	50	35	15
10	86.1	100	0	48	37	15

Table 3: Load share between the two generators for the configuration with and without TES - Amplitude $\Delta T = 4$ °C.

$\widetilde{T}_{ext}$ [°C]	E_{load}^{Daily} [kWh]	Load share without TES		Load share with TES		
		Heat Pump	**Boiler**	**HP to Load**	**HP to TES**	**Boiler**
5.5	101.4	56	44	38	34	28
7	96.3	64	36	47	36	17
8.5	91.2	64	36	40	41	19
10	86.1	72	28	48	37	15

Table 4: Load share between the two generators for the configuration with and without TES - Amplitude $\Delta T = 7.5$ °C.

5.5 Impact of the cost/efficiency coefficient

Since the optimal trajectory of the control variables $LF_{HP,j}$ and $LF_{B,j}$ (with $j = 1,..,N$) is strongly influenced by the coefficients of the cost function, which represent, for each considered technology (heat pump or gas boiler), the ratio between the prices of the energy vector in input to the system and the efficiency of the technology itself, a sensitivity analysis on the values of these coefficients has also been conducted. To this end, Eq. (12) has been reformulated as:

$$\min_{LF_{HP,j},LF_{B,j}} J = \frac{p_{gas}}{\eta_{boil}} \sum_{j=1}^{N} \left(k \frac{p_{el}}{p_{gas}} \frac{\eta_{boil}}{COP_j} Q_{HP}^{max} LF_{HP,j} + Q_B^{max} LF_{B,j} \right) \Delta t \quad (29)$$

In this way, we can consider either different energy price scenarios or different efficiencies for one or both the generators of the hybrid system, simply varying the value of the parameter k. For instance, the case with k=1.1 can represent either an increase of 10% of the electricity price or of the gas boiler efficiency, or a reduction of 10/1.1=9.1% of the heat pump COP or of the natural gas price. As reference case for the comparison of the results, the same configuration used for the previous analysis on the outdoor temperature profile is adopted. The results, reported in Tab. 1, highlight that cost savings significantly increase when k decreases, thus for a low ratio of electricity versus natural gas price or a high ratio of heat pump COP versus boiler efficiency. In other words, the potential of the hybrid system, when coupled with an optimally-controlled storage device, is exploited when the system powered by electric energy is much more convenient to be operated than the one burning natural gas, thanks to energy prices or to technological performances. It is interesting to observe that a reduction of the electricity price can be obtained with the introduction in the system of a renewable technology, such as photovoltaics, whose production of electrical energy can either be used directly to feed the heat pump or the electrical load of the building or be sold to the grid. In this latter case, the electricity price can be seen as the lost revenue for using that energy to feed the heat pump rather than selling it. Since the PV production varies over time, the resulting energy price profile will also be subject to the same variations, enabling the predictive control strategy to be even more effective.

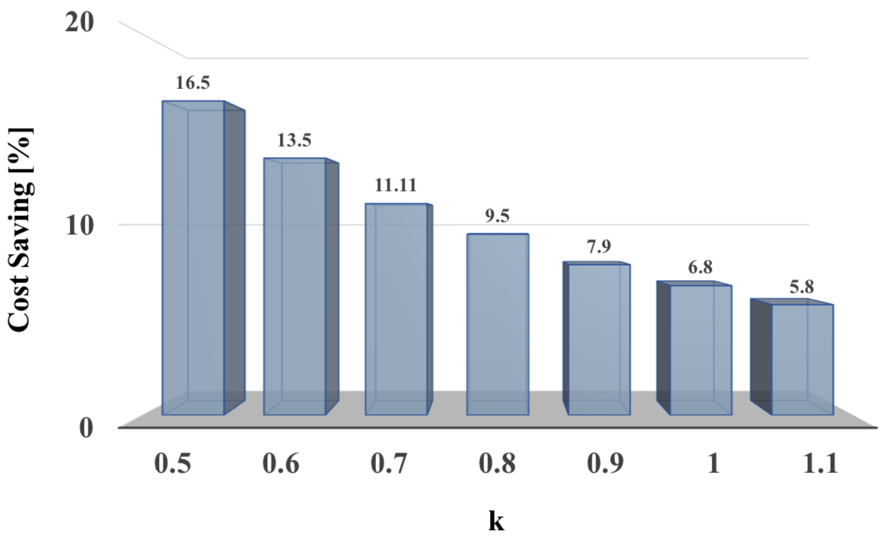

Figure 8: Impact of the cost/efficiency coefficient on the achievable cost saving.

6 Conclusions

The cost saving potential of an optimally-controlled hybrid generator composed by an air-to-water heat pump coupled with a gas boiler and a water-storage tank has been investigated. A model predictive control has been implemented to define the optimal control strategy of both generators. Furthermore, to fully explore the potential of the predictive controller, highlighting the relationship between the predictive ability and the storage capacity, the effects of different combinations of these parameters have been simulated in an ideal reference case scenario, in which the storage tank has been considered perfectly insulated. Results showed a reduction of the energy cost up to 8% with respect to a baseline scenario without storage capacity. Moreover, we showed a saturation effect of the cost saving with both the storage capacity and the predictive ability. A correlation between the optimal values of these two parameters has been highlighted. This correlation can be a handy design tool to determine the maximum prediction window useful to exploit a given storage volume or, vice-versa, the maximum useful storage volume with a given prediction window.

With the obtained optimal values of storage capacity and predictive ability, a sensitivity analysis of cost savings with respect to thermal losses of the storage tank has been performed. The effects of different external temperature profiles and of costs/efficiencies of the energy generators have been analysed as well. The hybrid system, coupled with an active thermal storage, can be an effective solution for demand side management, when MPC is implemented in the system (a specific analysis on the aspect of demand-response has been performed in [31]). Further control strategies and integration with solar technologies (thermal and photovoltaics) and electrochemical storage will be investigated in future works, looking for analogous correlations between optimal system sizing and prediction capabilities.

Acknowledgements

The authors would like to thank Prof. Walter Grassi, Mr. Davide Della Vista and Mr. Luca Urbanucci of DESTEC for the fruitful discussions about the system modelling and optimization. We gratefully acknowledge Immergas S.p.A. and, in particular, Mr. Cristian Zambrelli and Ms. Cristiana Bronzoni of the Research Centre, for letting us run the experimental campaign on their heat pump unit and in their climatic chamber.

Nomenclature

COP	Heat pump coefficient of performance
COP_{id}	Ideal heat pump coefficient of performance
COP_{eq}	Coefficient of performance of economic equivalence
CS	Cost saving [%]
CS_{max}	Maximum theoretical cost-saving [%]
c	Specific heat of water [kJ/kgK]
E_{load}^{daily}	Daily energy demand [kWh]
E_{useful}^{max}	Maximum storage energy [kWh]
LF_B	Boiler load factor
LF_B^{max}	Maximum boiler load factor
LF_B^{min}	Minimum boiler load factor
LF_{HP}	Heat Pump load factor
LF_{HP}^{max}	Maximum heat pump load factor
LF_{HP}^{min}	Minimum heat pump load factor
N	Prediction horizon [h]
p_e	Electricity price [€/kWh]
p_{gas}	Gas price [€/kWh]
$\dot{Q}_B$	Thermal power delivered by the boiler to the load [kW]
$\dot{Q}_B^{max}$	Maximum boiler thermal output [kW]
$\dot{Q}_{HP}^{max}$	Maximum heat pump thermal output [kW]
$\dot{Q}_{HP,L}$	Thermal power delivered by the heat pump to the load [kW]
$\dot{Q}_{HP,S}$	Thermal power delivered by the heat pump to the storage [kW]
$\dot{Q}_{S,L}$	Thermal power delivered by the storage to the load [kW]
$\dot{Q}_{load}$	Load demand [kW]
$\dot{Q}_{load}^{max}$	Peak load demand [kW]
$\dot{Q}_{loss}$	Storage losses to the surrounding [kW]
SC_{opt}	Best storage capacity
SoC	Storage state of charge
T_{cutoff}	Cut-off temperature [°C]
T_{des}	Design temperature [°C]
T_{em}	Emission system temperature [°C]

T_{ext}	Outdoor temperature [°C]
$\tilde{T}_{ext}$	Mean outdoor temperature [°C]
T_{off}	Switch-off temperature [°C]
T_s	Storage temperature [°C]
T_s^{max}	Maximum storage temperature [°C]
T_s^{min}	Minimum storage temperature [°C]
T_{sink}	Sink temperature [°C]
T_{source}	Source temperature [°C]
ΔT	Amplitude of the outdoor temperature profile [°C]
Δt	Time-step [h]
t	Time [h]
UA	Global heat transfer coefficient of the storage tank [W/K]
V	Storage tank volume [m^3]

Greek letters

β	Lift between the source and sink temperatures
δ_L	Binary variable
δ_S	Binary variable
η^{II}	Heat pump second law efficiency
η_{boil}	Boiler efficiency
ρ	Water density [kg/m^3]
τ	Dimensionless time horizon
τ_o	Reference time horizon [h]
ϕ	Building time shift [h]

References

[1] Eurostat. 2017. Consumption of energy, Statistics Explained website. Data extracted in June 2017: http://ec.europa.eu/eurostat/statistics-explained/index.php/Consumption_of_energy.

[2] European Parliament and Council. 2010. Directive 2010/31/EU on the energy performance of buildings. Brussels.

[3] European Parliament and Council. 2012. Directive 2012/27/EU on energy efficiency. Brussels.

[4] Bagarella, G., Lazzarin, R., Noro, M., 2016, Annual simulation, energy and economic analysis of hybrid heat pump systems for residential buildings. App. Therm. Eng. 99, 485-494.

[5] Bagarella, G., Lazzarin, R., Lamanna, B., 2013, Cycling losses in refrigeration equipment: an experimental evaluation, Int. J. Refrigeration 36 (8), 2111-2118.

[6] Bianco, V., Scarpa, F., Tagliafico, V., 2017, Estimation of primary energy savings by using heat pumps for heating purposes in the residential sector, App. Therm. Eng. 144, 938-947.
[7] Bagarella, G., Lazzarin, R., Noro, M., 2016, Sizing strategy of on-off and modulating heat pump systems based on annual energy analysis, Int. J. Refrigeration 65, 183 -193.
[8] Di Perna, C., Magri, G., Giuliani, G., Serenelli, G., 2015, Experimental assessment and dynamic analysis of a hybrid generator composed of an air source heat pump coupled with a condensing gas boiler in a residential building, App. Therm. Eng. 76, 86-97.
[9] Li, F., Zheng, G., Tian, Z., 2013, Optimal operation strategy of the hybrid heating system composed of centrifugal heat pumps and gas boilers, Energy and Buildings 58, 27-36.
[10] Scarpa, F., Tagliafico, L., Tagliafico, G., 2011, Integrated solar-assisted heat pumps for water heating coupled to gas burners; control criteria for dynamic operation, App. Therm. Eng. 31, 59-68.
[11] Qi, Z., Zao, Q., Liu, Y., Yan, Y., Spitler, J., 2014, Status and development of hybrid energy systems from hybrid ground source heat pump in china and other countries, Renewable and Sustainable Energy Reviews 29, 37-51.
[12] Renaldi, R., Kiprakis, A., Friedrich, D., 2017, An optimisation framework for thermal energy storage integration in a residential heat pump heating system, Applied Energy 186, 520–529.
[13] Pardo, N., Monter, A., Martos, J., Urchuegu, J.F., 2010, Optimization of hybrid-ground coupled and air-source-heat pump systems in combination with thermal storage, App. Therm. Eng. 30 (8-9), 1073-1077.
[14] Yu, Z.J., Huang, G., Haghighat, F., Hongqiang, L., Zhang, G., 2015, Control strategies for integration of thermal energy storage into buildings: State-of-the-art review, Energy and Buildings 106, 203-2015.
[15] T.Y. Chen, Application of adaptive predictive control to a floor heating system with a large thermal lag, Energy and Buildings 34 (2002) 45-51.
[16] Cho, S.H., Zaheer-uddin, M., 2003, Predictive control of intermittently operated radiant floor heating systems, Energy Conversion and Management 44, 1333–1342.
[17] H. Karlsson, C.-E. Hagentoft, Application of model based predictive control for water-based floor heating in low energy residential buildings, Building and Environment 46 (2011) 556-569.
[18] Hewitt, N.J., 2012, Heat pumps and energy storage - The challenges of implementation, Applied Energy 89.1, 37-44.
[19] Arteconi, A., Hewitt, N. J., and Polonara, F., 2012, State of the art of thermal storage for demand-side management, Applied Energy 93, pp. 371–389.
[20] Arteconi, A., Hewitt, N.J., Polonara, F., 2013, Domestic demand-side management (DSM): Role of heat pumps and thermal energy storage (TES) systems, App. Therm. Eng. 51.1-2, 155–165.
[21] Verhelst, C., Logist, F., Van Impe, J., Helsen, L., 2012, Study of the optimal control problem formulation for modulating air-to-water heat pumps connected to a residential floor heating system. Energy and Buildings, 45, 43-53.
[22] Verhelst, C., Axehill, D., Jones, C.N., Helsen, L., 2010, Impact of the cost function in the optimal control formulation for an air-to-water heat pump system, 8th International Conference on System Simulation in Buildings, Liege, December 13-15.
[23] Schütz, T., Streblow, R., Müller, D., 2015, A comparison of thermal energy storage models for building energy system optimization, Energy and Buildings 93, 3-31.
[24] Cole, W.J., Morton, D.P., Edgar. T.F, 2014, Optimal electricity rate structure for peak demand reduction using economic model predictive control, J. Process Control 24 (8), 1311-1317.
[25] Oldewurtel, F., Pariso, A., Jones, C.N., Gyalistras, D., Gwerder, M., Stauch, V., Lehmann, B., Morari, M., 2012, Use of model predictive control and weather forecasts for energy efficient building climate control, Energy and Buildings 45, 15-27.
[26] Sturzenegger, D., Gyalistras, D., Morari, M., Smith, R.S., 2016, Model predictive climate control of a swiss office building: implementation, results, and cost-benefit analysis, IEEE Trans. Control Syst. Technol. 24 (1), 1-12.

[27] Halvagaard, R., Bacher, P., Perers, B., Andersen, E., Furbo, S., Jørgensen, J.B., Poulsen, N.K., Madsen, H., 2012, Model predictive control for a smart solar tank based on weather and consumption forecasts, Energy Procedia 30, 270-278.
[28] EN 15603:2008, "Energy Performance of Buildings – Overall Energy Use and Definition of Energy Ratings", CEN (European Committee for Standardization), Brussels, Belgium, 2008.
[29] Testi, D., Schito, E., Conti, P., 2016, Cost-optimal sizing of solar thermal and photovoltaic systems for the heating and cooling needs of a nearly Zero-Energy Building: design methodology and model description, Energy Procedia 91, 517-527.
[30] Testi, D., Schito, E., Conti, P., 2016, Cost-optimal sizing of solar thermal and photovoltaic systems for the heating and cooling needs of a nearly Zero-Energy Building: the case study of a farm hostel in Italy, Energy Procedia 91, 528-536.
[31] D'Ettorre, F., De Rosa, M., Conti, P., Schito, E., Testi, D., Finn, D. P., 2018, Economic assessment of flexibility offered by an optimally controlled hybrid heat pump generator: a case study for residential building, Energy Procedia 148, 1222- 1229.
[32] EN 14511-2:2011, "Air Conditioners, Liquid Chilling Packages and Heat Pumps with Electrically Driven Compressors for Space Heating and Cooling – Part 2: Test Conditions", CEN (European Committee for Standardization), Brussels, Belgium, 2011.
[33] EN 15316-4-2:2008, "Heating Systems in Buildings – Method for Calculation of System Energy Requirements and System Efficiencies – Part 4-2: Space Heating Generation Systems, Heat Pump Systems", CEN (European Committee for Standardization), Brussels, Belgium, 2008.

Appendix A. Experimental characterization of the heat pump performances

To characterize the heat pump behaviour, an experimental campaign has been conducted in a climatic chamber, in which the heat pump operation has been investigated under different working conditions. The set-up of the experimental apparatus in the climatic chamber is reported in Fig. A.1.

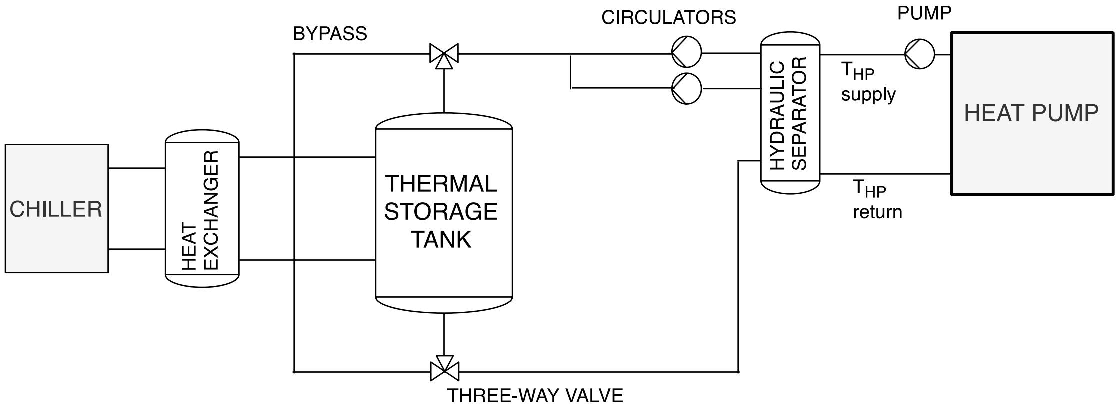

Figure A.1: Experimental apparatus in the climatic chamber.

A.1 Set-up of the experimental apparatus

An 8-kW heat pump is connected by means of a primary hydraulic circuit to a hydraulic separator, from which a secondary hydraulic circuit is derived, to connect the hydraulic separator to a cold-water storage tank, which emulates the building thermal load. The flow rate in the primary circuit is kept constant and equal to 1.2 m^3/h, while its temperature can be varied, acting directly on the heat pump electronic controller. In the secondary circuit, the flow rate can be varied between 0.3 and 0.6 m^3/h, operating one or both the circulators located downstream of the manifold, according to the building thermal load to be simulated. Part of the ongoing flow from the manifold is then sent to the water storage tank, which is kept at a constant temperature of 10 °C by means of a chiller, while the other part of the flow by-passes the storage by means of a three-way valve. The water exiting the storage tank is properly mixed with the by-passed flow, in order to achieve the desired return temperature to the manifold and, consequently, to the heat pump. Furthermore, to emulate different outdoor temperature conditions, the temperature inside the climatic chamber has been varied by means of an air handling unit. All the system control implementation and data acquisition are realized by the software LabView™. All the measurement errors are within the limits allowed by standard EN 14511-2:2011 [32].

A.2 Test conditions

To emulate different heat pump working conditions, the supply temperature, the external temperature profile, and the required thermal power have been varied in the ranges: 30-55 °C, 0-11 °C, and 4-10 kW.

A.3 Correlation

As suggested by several technical standards (see, for instance, EN 15316-4-2 [33]), the so-called second-law efficiency (η^{II}) is used to evaluate the heat pump performance. The latter reads:

$$COP = \eta^{II} COP_{id} \qquad \text{(A.1)}$$

where COP_{id} is the coefficient of performance of a reversed Carnot cycle (temperatures in kelvins):

$$COP_{id} = \frac{T_{sink}}{T_{sink} - T_{source}} \quad \text{(A.2)}$$

The source temperature (T_{source}) is considered equal to the air temperature inside the climatic chamber (T_{ext}), while the sink temperature is considered as the mean between the supply and the return water temperature from/to the manifold connected to the heat pump. Finally, to evaluate the second low efficiency η^{II}, taking into account the effects of both the lift between the source and sink temperatures and the part load conditions, the polynomial correlation (A.5) has been used, based on the dimensionless parameters:

$$\beta = \frac{T_{sink}}{T_{source}} \quad \text{(A.3)}$$

$$LF_{HP} = \frac{\dot{Q}_{HP}}{\dot{Q}_{HP}^{max}} \quad \text{(A.4)}$$

$$\eta^{II} = c_0 + c_1\beta + c_2 LF_{HP} + c_3\beta^2 + c_4\beta LF_{HP} \quad \text{(A.5)}$$

β is the ratio between the source and sink temperatures and is correlated to the compression ratio of the heat pump compressor, while LF_{HP} is the load factor of the heat pump. The latter is correlated to the compressor frequency and it is considered equal to the ratio between the thermal power delivered by the heat pump $\dot{Q}_{HP}$ and its maximum power $\dot{Q}_{HP}^{max}$).
Finally, the coefficients of the polynomial expression, reported in Tab. A.1, have been obtained minimizing the difference between the measured electrical powers absorbed by the heat pump during the tests and the ones evaluated by means of the above correlation.

$c_0 = -19.42$	$c_1 = 33.71$	$c_2 = 1.33$	$c_3 = -14.42$	$c_4 = -1.081$

Table A.1: Coefficients of the polynomial expression (A.5).

Results are reported in Fig. A.2 and show a good agreement between the measured COP values (15600 experimental points) and the ones evaluated by the correlation, under the same operative conditions.

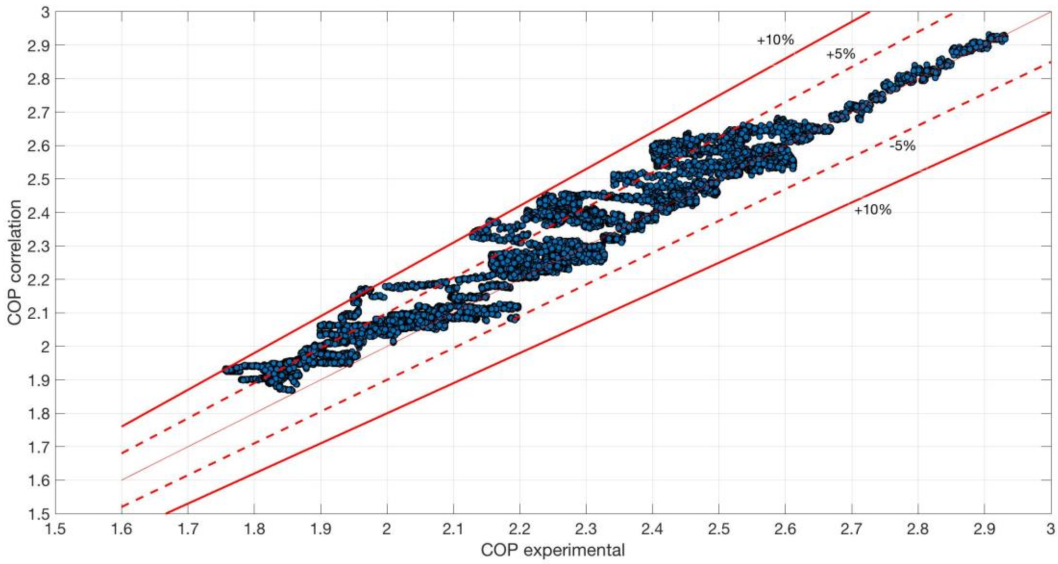

Figure A.2: Correlation vs. experimental COP (red continuous: 10% relative error bounds; red dashed: 5% relative error bounds).